
Simulating Wildfire Containment with Realistic Tactics

Jeremy S. Fried and Burton D. Fried

ABSTRACT. Existing simulation models for fire protection planning rely on a containment algorithm which fails to account for the interaction between the production of containment line and a fire's capacity to spread. This paper describes a technique for simulating wildland fire containment which explicitly accounts for this interaction by extending, generalizing, and, in some cases, simplifying methods reported earlier (Anderson 1983, Albini et al. 1978, Mees 1985, Anderson 1989). Representing the containment boundary in parametric form [i.e., expressing its Cartesian (x, y) or polar (r, θ) coordinates as functions of a dimensionless parameter instead of specifying y as a function of x or r as a function of θ], leads to a formalism with two significant advantages: (1) it allows a free choice for the shape of the free burning fire boundary, and (2) it is appropriate for simulations of parallel (indirect) attack as well as direct head and tail attack. In general, the technique requires solution of a first-order, nonlinear, differential equation, a task easily accomplished using numerical methods. The dependence of final fire size and containment time on the line-building rate and eccentricity of the free burning fire boundary are illustrated with the special case of an expanding ellipse and constant line-building rate, for which the containment boundary can be obtained by a simple quadrature.

Our General Formulation algorithm is demonstrated with a series of simulations that span the range of likely parameters for fire spread and fireline production. Comparisons made on representative fires between predictions of the General Formulation and models currently in use indicate that current models almost always overestimate fire size, sometimes by as much as an order of magnitude. *For. Sci.* 42(3):267-281.

Additional Key Words. Initial attack suppression modeling.

Wildland fires, which annually consume millions of acres of forest and watershed (sparsely populated areas covered with some kind of vegetation, usually grass or chaparral) in North America alone, are typically fought with a combination of firefighting resources such as water-carrying fire engines, bulldozers, crews carrying hand tools, and water-dropping aircraft. The primary goal is the earliest possible containment of fire spread, generally by deprivation of combustible fuel and oxygen at the fire perimeter. This goal is most commonly (and efficiently) achieved by rapid encirclement of the fire with a fireline, a strip (whose width depends on the intensity of the fire) either cleared of all readily combustible material or sufficiently wetted to make combustion unlikely. This critical phase of firefighting, usually requiring no more than 8 hours, and far less in many cases, is called "initial attack."

In practice, firefighters choose and deploy initial attack strategies and tactics that are best suited to firefighting objectives and the particular conditions of the fire that they are fighting. Final fire size is usually minimized by a direct attack strategy, in which fireline is constructed on the flaming front, the region where combustible fuels are igniting. Direct attack is often described by firefighters as having "one foot in the green and one in the black." Initiating fireline construction at the head of a fire (rather than the tail) is a tactic that can result in smaller fires since the portion of the fire perimeter that is spreading the fastest is halted first. However, with high intensity and fast spreading fires, both of these approaches have the potential for serious injuries or fatalities when firefighters are overrun. In such cases, it is common to use a parallel (indirect) attack strategy, in which fireline is constructed parallel to, but at a safe distance (offset) away from, the

Jeremy S. Fried is Assistant Professor at the Department of Forestry, Michigan State University, East Lansing, MI 48824, and Burton D. Fried is Professor Emeritus at the Department of Physics, University of California, Los Angeles, CA 90024.

Acknowledgments. The authors gratefully acknowledge support arranged by Wayne Mitchell under Interagency Agreement 7CA74631 between the California Department of Forestry and Fire Protection and The University of California and the suggestions of reviewers Frank Albini and David Anderson which greatly improved this manuscript.

fire perimeter, often in conjunction with setting “back-fires” (also known as “firing out”).

Simulation of the initial attack process currently plays an important role in fire protection planning and budgeting at the state and federal levels and has the potential to improve firefighter training. It may also prove important for landscape level modeling efforts that support ecosystem management in areas where fire is an active agent of ecosystem transformation. In all of these applications, it is useful, if not essential, to explore the likely impacts of changes in the state and decision variables which define the system (e.g., the strength and location of fire protection forces, dispatching rules, prescribed burning, or other vegetation management) via a modeling approach because the opportunities for experimental manipulation are limited, at best. If reliable inferences are to be drawn from such modeling efforts involving the wildland fire system, it is critical that the underlying simulation of initial attack mimic the actual fire suppression process as closely as possible, and that it be flexible enough to distinguish among alternative, real-world variations in firefighting tactics. The model must lend itself to sufficiently rapid computation that it is economically feasible to simulate a large variety of conditions, making possible a sound statistical analysis, and it must have sufficient accuracy to make the conclusions drawn from the simulations a reliable basis for planning and resource allocation.

Existing simulation models of initial attack effectiveness, widely used by state and federal fire agencies for budgeting and planning initial attack deployment, have usually relied on an oversimplified representation of fire containment in which line construction and perimeter growth are computed independently and containment occurs when the total length of constructed fireline equals the total length of the perimeter (e.g., USDA Forest Service 1985, Fried and Gillies 1988). For example, in the National Fire Management Analysis System (NFMAS) currently used throughout the National Forest System for fire protection planning and budget justification, all fires are assumed to be ellipses with a 2:1 length to width ratio, and to retain that shape, burning freely, right up until the moment when an optimally positioned, encircling ellipse of fireline, built from the tail towards the head, is closed. At that instant, the fire, for the first time, contacts the encirclement line, and does so around the entire perimeter of the fire. This “conventional approach” is insensitive to the timing of resource arrivals, fails to accommodate the analysis of alternative tactics and strategies, and commonly overestimates burned area by as much as an order of magnitude.

To achieve the goals described above for a successful and useful simulation model, two improvements over the models in current use appear to be desirable: (1) the ability to have variations in line-building rate comparable to those which occur in practice, and (2) a formulation which takes into account the interaction between advance of the fire and the line-building work throughout the course of the fire suppression.

Earlier Work

The work reported here represents an extension and generalization of earlier studies on the mathematical analysis of fire suppression, which began with the seminal 1978 paper of

Albini, et al. (first published in Russian in 1977). In that paper, it was assumed that: (1) the free burning fire boundary (fbfb) is a smooth curve which evolves over time in a self-similar fashion, (2) the rate of expansion of the fbfb is constant, (3) the rate of fireline construction is constant, (4) fireline is built symmetrically (i.e., the line-building rate is the same for the upper and lower portions of the boundary), and (5) the fbfb has a particular shape, involving powers of trigonometric functions. (A general formulation not requiring assumptions 2 through 5 is presented, but the detailed analysis makes use of these assumptions.)

The authors first study the case of direct attack using a “self-consistent” analysis in which the line-building effort provides, from the start, some containment and the evolution of the uncontained portion of the fbfb determines the direction of the line-building effort at each instant. They also analyze a particular model of indirect attack, wherein a line perpendicular to the direction of advance of the fire is constructed at a distance d from the head of the fire and, when the fire reaches that line, the line building proceeds toward the fire at such an angle that it is tangent to the fbfb when the two meet. Thereafter, direct attack is used. The optimum value of d is obtained by numerical examination of the dependence of the final fire area and its perimeter on d .

A 1983 paper by H. Anderson provides an extensive study of the fbfb shapes, using data from pine litter fuel beds burning in a wind tunnel as well as field measurements. On the basis of his own work as well as a number of earlier papers, he concluded that a satisfactory representation of real fbfb's is provided by a “double ellipse,” i.e., two conjoined, oppositely facing semi-ellipses, of different eccentricity and focal length, with the origin of the fire at one focus. Anderson's work is extremely valuable when, in calculations like Albini's and subsequent studies, a choice of fbfb shape must be made.

A 1985 paper by Mees retained Albini's assumptions 1 and 2 but dropped 3 and 4, i.e., considered variable line construction rates, different in general, for the upper and lower parts of the boundary. Also, in place of Albini's trigonometric power shape for the fbfb, Mees assumed an ellipse with the fire at one focus. His analysis of the direct attack was, like Albini's, self-consistent, and, in general, equivalent to Albini's, save for the greater generality afforded by the elimination of assumptions 3 and 4. Mees termed the self-consistent approach “complex,” to distinguish it from a “simple” model, introduced in that paper, in which the fbfb is allowed to evolve with no containment until the time t_c when its perimeter is equal to the perimeter of an elliptical fireline constructed at the given (variable) line-building rate. Thus, there is no interaction between the fireline and the fbfb until the time t_c when the fire is suddenly and completely contained. Since this Simple Method significantly reduces the computational effort required, it is used in simulation models widely relied upon by state and federal fire agencies for budgeting and planning initial attack deployment. However, as we will show, it does not give a sufficiently accurate representation of the results obtained with the more realistic self-consistent approach.

In 1989, D. Anderson used a self-consistent formulation to study the case of direct attack, retaining the first four of Albini's assumptions but using for the fbfb shape an ellipse, expanding at a constant rate around a center moving towards the head of the fire at a constant speed. He also considered a model of indirect attack, which differs from Albini's in that after the fire reaches the perpendicular fireline, the direction of subsequent line building is perpendicular to the initial fireline (i.e., antiparallel to the direction of advance of the fire.) With this model, he was able to solve analytically for the optimum value of the distance d at which the perpendicular line should be constructed.

Approach

This work aims to extend, generalize, simplify, and unify these earlier studies, the goal being to formulate an algorithm which, taking advantage of the enhanced computational facilities that have become widespread in forestry since those early papers, leads to sufficiently rapid computation that it is economically feasible to simulate a large variety of conditions, making possible a sound statistical analysis, and yet has sufficient accuracy and flexibility to make the conclusions drawn from the simulations a reliable basis for planning and resource allocation.

Of Albini's simplifying assumptions, we retain only the first. Thus, while the fbfb evolves in a self-similar fashion, it may do so at a variable rate and the shape can be chosen arbitrarily. In particular, any of the models used in the papers cited above (Albini's trigonometric power functions, H. Anderson's single and double ellipses with the fire at one focus, D. Anderson's ellipse with moving center, etc.) can be readily implemented. The line construction rates on the upper and lower boundaries are independent, and each can be an arbitrary function of time. Some analytic simplification is achieved by formulating the problem in rectangular (x, y) coordinates, rather than the polar coordinates (r, θ) used in the earlier papers, and using a parametric representation of the fbfb in terms of a parameter u , chosen to facilitate the analysis, rather than θ . As a result, we find that the analysis leads to a quite tractable algorithm, notwithstanding the relaxation of Albini's assumptions 2 through 5. As an illustrative (and important) example we shall use an elliptical fbfb in specific calculations, but the formulation applies equally well to other shapes.

The results are greatly simplified when the ratio of line

construction rate V to fbfb expansion velocity V_h , $\left(P = \frac{V}{V_h} \right)$

is constant. For any choice of fbfb shape, the calculation of containment time and area burned then reduces to a simple quadrature, facilitating an analysis of the sensitivity of the initial attack process to variations in the parameters of the problem. In the particularly simple case of a circular fbfb with constant P , simple analytic expressions for both containment time and area are obtained, and these turn out to be exponential functions of $\frac{1}{\sqrt{P^2 - 1}}$. (For other shapes, a qualitatively similar dependence on P is observed.)

similar dependence on P is observed.)

A completely new feature of the present work is the analysis of a method of indirect attack quite different from those of Albini and D. Anderson. If fireline is constructed at a constant distance L from the fbfb, the problem reduces to that of direct attack on a fire whose boundary is a distance L from the actual fbfb. The analysis goes through without difficulty, even though this "super fbfb," as we call it, does not evolve in a self-similar manner.

Analysis

The Free Burning Fire Boundary (fbfb)

Consistent with earlier work on this problem (Albini et al. 1978, Anderson 1983, Anderson 1989, Mees 1985), it is assumed here that the fbfb can be characterized by some specified shape which expands in a self-similar way as time progresses. In the absence of wind, sloped land, or anisotropic distribution of fuel, the fbfb would be a circle. With any of those factors present, the fbfb is elongated. The simplest representation is then an ellipse, whose eccentricity is determined by the prevailing wind velocity, slope, etc., but other, more complex choices of fbfb shape have been suggested (Anderson 1983, Albini et al. 1978). For any choice of fbfb shape, the boundary at time t can be represented in Cartesian coordinates as

$$x = h(t)X(u, \epsilon) \quad y = h(t)Y(u, \epsilon) \quad (1)$$

where $x = y = 0$ is the origin of the fire; u is an angle-like variable whose domain we can choose to be $0 \leq u \leq 2\pi$; and $h(t)$ is a monotonically increasing function of time which sets the scale size for the fbfb. Figure 1 shows an elliptical fbfb with h chosen as the distance from the origin of the fire to the head. X and Y are dimensionless functions of u and ϵ , where ϵ denotes one or more parameters which characterize the fbfb shape.¹

The x axis is chosen to be in the direction of the wind, slope, or fuel gradient, so the head of the fbfb is at the right, the tail at the left. It is always possible to normalize u so that $u = 0$ corresponds to the head of the fire, and $u = \pi$, to the tail. Then for a given value of t , the point (x, y) given by (1)

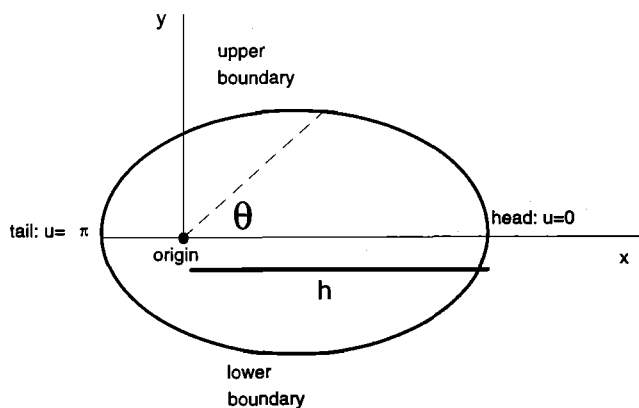


Figure 1. An elliptical representation of a free-burning fire boundary for a prototypical wildfire.

traverses the fbfb in a counter-clockwise direction, starting at the head, as u goes from 0 to 2π . As t increases, the fbfb expands, but with fixed shape, i.e., in a self-similar manner.

Simulation of Containment

In simulating direct attack, it is assumed that the fire originates at time $t = 0$ and burns freely, with a boundary determined by (1), until the time t_0 when the first line-building resources arrive at some point on the perimeter (typically, but not necessarily, the head or tail of the fire). Starting from that point, line is built in both the clockwise and counter-clockwise directions until the fire is contained or until it outruns the line-building effort and is considered to have escaped. A fire may also be considered to have escaped initial attack if its containment time exceeds t_{\max} or its size, $Area_{\max}$. These escape limits are somewhat situation specific and are intended to account for the fact that for an actual fire, neither ambient burning conditions nor fire shape will remain constant indefinitely. (For example, when the fire crosses a ridge, the slope, wind velocity, both magnitude and direction, and fuel composition may change.) Moreover, it is likely that after some time (1–8 hours), extended attack resources (as opposed to initial attack resources) will be dispatched to the incident and a different set of firefighting strategies and tactics adopted.

Fireline is rarely built at a constant rate for the duration of an initial attack effort. After an initial attack begins following the arrival of the first firefighting resource, aggregate productivity increases incrementally with the arrival of each additional resource and decreases as resources exhaust their supplies of water and the energies of their crews. The net result is a production rate “stairstep” (up and down) over time (Figure 2).

The case of parallel or indirect attack can be modeled by assuming that line is built so as to contain a super “fbfb,” defined as the locus of points (outside the fbfb) for which the shortest, straight-line distance to a point on the actual fbfb is some chosen offset distance L . The parallel attack problem is then similar to that for direct attack but with the fbfb replaced by the super fbfb. (Note that the super fbfb does not evolve in a self-similar manner since the ratio of L to h is, in general, not constant.)

For the sake of clarity, the simplest case, namely direct tail attack, will be discussed. The extension to other cases of interest, such as direct, head attack, and parallel attack (head or tail) is then quite straightforward. Initially, the problem is formulated and a solution derived for the general case (i.e., with no specific choice for the fbfb shape). This formalism is then applied to the specific example of an elliptical fbfb.

Resource	Response time (min.)	Production rate (chains/hour)	Drop-off distance (feet)	Post-drop-off production (chains/hour)
Engine #1	6	5	120	3
Engine #2	12	5	180	3
Bulldozer #1	15	7	NA	NA

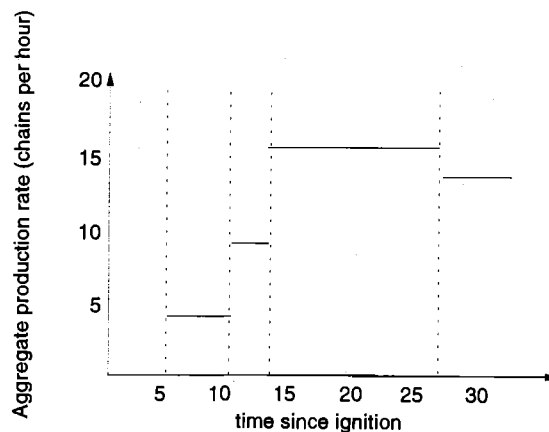


Figure 2. Example of how a dispatch list translates to production rate over time. The “drop-off” distance is the length of line that can be constructed before crews become fatigued or water or retardant are depleted; the “post-drop-off production” is the rate that can be maintained after this drop-off phenomenon has occurred.

Direct Tail Attack

Line building starts at the tail at time $t = t_0$ and proceeds in both clockwise and counter-clockwise directions, not necessarily at the same rate. At time t , the points of furthest advance of the line building on the "upper" and "lower" (in xy space) portions of the boundary are characterized by the values $u = u_1(t)$ and $u = u_2(t)$, respectively. It is convenient to label these points Q_1 and Q_2 , i.e., Q_i is the point with coordinates $x_i = hX(u_i, \epsilon)$, $y_i = hY(u_i, \epsilon)$. At time t_0 , when the first resources arrive at the tail of the fire, the points Q_1 and Q_2 coincide. As time progresses they move apart, Q_1 advancing in a clockwise direction along the upper portion of the boundary while Q_2 moves in a counter-clockwise direction along the lower portion of the boundary. If Q_1 and Q_2 meet at a later time t_c which is less than some preassigned time t_{max} , the fire is considered to be contained, and the containment time is t_c . Q_1 and Q_2 will eventually meet *unless* one or both of the line-building efforts are unable to keep up with the fbfb (so that firefighters at the head of the line-building activity would be overwhelmed by flames from all sides). Should that happen, the fire is classified as having escaped, and, as indicated above, the same classification is also applied if Q_1 and Q_2 have not met prior to t_{max} .

If the fire is contained, the parametric equations for the upper containment boundary are

$$x = x_1(t) \equiv h(t)X[u_1(t), \epsilon], \quad y = y_1(t) \equiv h(t)Y[u_1(t), \epsilon] \quad (2)$$

where t , considered as a parameter, ranges over the interval $t_0 \leq t \leq t_c$, and $x = X(u, \epsilon)$, $y = Y(u, \epsilon)$ are parametric equations for the chosen fbfb shape. The equations for the lower containment boundary are analogous:

$$x = x_2(t) \equiv h(t)X[u_2(t), \epsilon], \quad y = y_2(t) \equiv h(t)Y[u_2(t), \epsilon] \quad (3)$$

and the area of the contained fire is given by

$$Area = \int_{t_0}^{t_c} y_1(t) \frac{dx_1}{dt} dt - \int_{t_0}^{t_c} y_2(t) \frac{dx_2}{dt} dt \quad (4)$$

Since h , the size scaling factor for the free burning fire, is a prescribed, monotonically increasing function of time $h(t)$, this function could be inverted to obtain $t(h)$, so we are free to use h as an independent variable in place of t . (Although not an essential element of the analysis, this step leads to some simplifications in the algebra that follows.) With h as independent variable, (2), (3) and (4) are replaced by

$$x = x_1(h) \equiv hX[u_1(h), \epsilon], \quad y = y_1(h) \equiv hY[u_1(h), \epsilon], \quad (5)$$

$$h_0 \leq h \leq h_c$$

$$x = x_2(h) \equiv hX[u_2(h), \epsilon], \quad y = y_2(h) \equiv hY[u_2(h), \epsilon], \quad (6)$$

$$h_0 \leq h \leq h_c$$

$$Area = \int_{h_0}^{h_c} y_1(h) \frac{dx_1}{dh} dh - \int_{h_0}^{h_c} y_2(h) \frac{dx_2}{dh} dh \quad (7)$$

where $h_0 = h(t_0)$ and $h_c = h(t_c)$.

The central problem of the simulation is to determine the functions $u_1(t)$ and $u_2(t)$, or, equivalently, $u_1(h)$ and $u_2(h)$. Differential equations for these functions are obtained by requiring that the speed of advance of the points where line is being built,

$$v = \frac{dh}{dt} = \sqrt{\left(\frac{dx}{dt}\right)^2 + \left(\frac{dy}{dt}\right)^2} \quad (7.1)$$

$$= \sqrt{\left[V_h X + h\left(\frac{dX}{du}\right)\left(\frac{du}{dt}\right)\right]^2 + \left[V_h Y + h\left(\frac{dY}{du}\right)\left(\frac{du}{dt}\right)\right]^2}$$

should just match the line-building capacity of the available resources.²

Let V_1 and V_2 be the line-building rates on the upper and lower boundaries. Then for the upper boundary

$$\left(\frac{dx}{dt}\right)^2 + \left(\frac{dy}{dt}\right)^2 = V_1^2 \quad (8)$$

or, dividing by $V_h^2 \equiv \left(\frac{dh}{dt}\right)^2$,

$$\left(X + hX_u \frac{du_1}{dh}\right)^2 + \left(Y + hY_u \frac{du_1}{dh}\right)^2 \equiv \left(\frac{V_1}{V_h}\right)^2 \equiv P_1^2 \quad (9)$$

where X_u and Y_u denote partial derivatives of X and Y with respect to u and $P_1(h)$ is the ratio of the line-building rate for the upper boundary to the expansion rate of the free burning fire, V_h . (Since V_1 and V_h are given functions of t , P_1 is a known function of t or, equivalently, of h .) An equation exactly similar to (9), with the subscripts 1 replaced by subscripts 2, describes the lower boundary. In (9) and its companion for the lower boundary, we have two quadratic equations for the derivatives $\frac{du_i}{dh}$, with $i = 1, 2$.

Solving these gives

$$\frac{du_i}{dh} = \frac{-(XX_u + YY_u) \pm \sqrt{P_i^2(X_u^2 + Y_u^2) - (X_u Y - Y_u X)^2}}{h(X_u^2 + Y_u^2)} \quad (10)$$

For reasons explained later, the negative sign on the square root should be used for the upper boundary ($i = 1$) and the positive sign for the lower boundary ($i = 2$).

Since X and Y are given functions of u and ϵ , while P_i is a known function of h , (10) constitutes two ordinary, first-

order differential equations for the functions $u_i(h)$ which can be solved by standard techniques, e.g., Runge-Kutta integration (Press et al. 1986). In carrying out the integration, the distance

$$D = \sqrt{[x_1(h) - x_2(h)]^2 + [y_1(h) - y_2(h)]^2}$$

between the points Q_1 and Q_2 must be calculated at each step. As noted earlier, D is initially zero but increases with time as h increases and Q_1 and Q_2 move apart. If the fire can be contained by the resources assumed, then Q_1 and Q_2 will converge and D will again be zero at some time t_c corresponding to $h = h_c$. If t_c is less than some previously assigned value, t_{\max} , the fire is classified as contained and t_c is the containment time; otherwise, the fire is classified as having escaped.

It can be shown that escape due to inadequate line-building rates will occur if, at any time, P_1 or P_2 becomes less than $\sqrt{X^2 + Y^2}$ or equivalently, $\frac{du_i}{dt}$ changes sign.³ Accordingly, if at any time step in the integration procedure, P_1 or P_2 falls below $\sqrt{X^2 + Y^2}$ and $\frac{du_i}{dt}$ changes sign, the integration is stopped and that fire is classified as having escaped.

Before discussing direct head attack and indirect attack, three useful special examples of direct tail attack will be considered: (a) the case where the P_i are constant and the integration of (10) reduces to a simple (numerical) quadrature; (b) the case of an elliptical fbfb.; and (c) the case of a circular fbfb with constant P_i .

Constant P_i

In this case, the only h dependence on the right hand side of (10) comes from the factor h in the denominator. It follows that (10) can be written in the form

$$\frac{du_i}{dh} = \frac{f(u_i)}{h} \quad (13)$$

with

$$f(u_i) = \frac{-(XX_u + YY_u) \pm \sqrt{P_i^2(X_u^2 + Y_u^2) - (X_u Y - Y_u X)^2}}{(X_u^2 + Y_u^2)} \quad (14)$$

and that

$$\log\left(\frac{h}{h_0}\right) = \int_{\pi}^{u_i(h)} \frac{du}{f(u)} \equiv g(u_i) \quad \text{or} \quad h = h_0 e^{g(u_i)} \quad (15)$$

Thus, h is obtained as a function of u_i , or, inverting, u_i as a function of h , by simply carrying out the definite integral in (15). In general, this integration must be done numerically,

but the computation is still minimal compared to the integration of the differential equation (10).

Although this is, admittedly, a special and simple case, the result (15) is nevertheless useful as a check on the algorithm outlined above for the general case of variable P_i . Moreover, this approach can be extended to the case where P_i is piecewise constant, i.e., when discrete resources arrive at specified times. If P_i has the constant value P for a range of t or h given by $h_a \leq h \leq h_b$, (13) gives

$$\log \frac{h}{h_a} = \int_{u_a}^{u_i(h)} \frac{du}{f(du)} \quad h_a \leq h \leq h_b \quad (16)$$

where $u_a = u_i(h_a)$. By repeated application of (16), $u_i(h)$ could be determined over the whole range $h_0 < h < h_c$, without the necessity of resorting to Runge-Kutta or other integration procedures. However, in practice, dealing with the escape conditions and with the determination of h_c as the value for which D vanishes makes this approach less attractive than one might initially suppose. In the authors' experience, the more straightforward approach of integrating (10) by standard methods is simpler to implement, even for the case of piecewise constant P_i .

Elliptical fbfb

Of the various models for the fbfb shape cited earlier, the simplest is an ellipse, with one focus at the origin of the fire and the major axis parallel to the wind or gradient direction. Although some of the other models may better represent individual fires, the comparisons shown by Anderson (1983) between actual fire boundaries and those obtained using his double ellipse model suggest that the variation among models is typically less than the discrepancies between the predictions of any model and actual fire boundaries. The relative simplicity of the elliptical model makes it a good choice for simulating a series of fires under a variety of conditions.

Using coordinates with origin at the left-hand focus,⁴ the parametric equations for the ellipse then become

$$x = h \frac{\cos u + \epsilon}{1 + \epsilon} \quad y = hA \sin u \quad A \equiv \sqrt{\frac{1 - \epsilon}{1 + \epsilon}} \quad (21)$$

In the notation of (1) it follows that the functions X and Y are given by

$$X(u, \epsilon) = \frac{\cos u + \epsilon}{1 + \epsilon} \quad Y(u, \epsilon) = A \sin u \quad (22)$$

Calculating X_u and Y_u and substituting these in (10) gives, after some straightforward algebra,

$$\frac{du_i}{dh} = \frac{\epsilon \sin u_i \pm (1 + \epsilon) \sqrt{P_i^2 \frac{1 - \epsilon \cos u_i}{1 + \epsilon \cos u_i} - A^2}}{h(1 - \epsilon \cos u_i)} \quad (23)$$

It only remains to carry out the numerical solution of these two differential equations, e.g., using Runge-Kutta integration, and, following the algorithm given below, compute t_c and the fire area.

Circular fbfb

In general, the computation of containment time and area must be carried out numerically, but for the special case where P_i is constant and $\epsilon = 0$ (circular fbfb shape), it is possible to obtain analytic expressions for both t_c and the area. When $\epsilon = 0$, (23) reduces to

$$\frac{du_i}{dh} = \pm \frac{\sqrt{P_i^2 - 1}}{h} \quad (24)$$

and this can be integrated for constant P_i , giving

$$u_1 = \pi - \sqrt{P_1^2 - 1} \log \frac{h}{h_0} \text{ and } u_2 = \sqrt{P_2^2 - 1} \log \frac{h}{h_0} \quad (25)$$

Containment occurs when the two line-building efforts reach a common point on the boundary, i.e., when $u_2 = u_1 + 2\pi$. The associated h value, h_c , is given by

$$\left(\sqrt{P_1^2 - 1} + \sqrt{P_2^2 - 1} \right) \log \frac{h_c}{h_0} = 2\pi \quad (26)$$

or

$$h_c = h_0 e^{\left(\frac{2\pi}{\sqrt{P_1^2 - 1} + \sqrt{P_2^2 - 1}} \right)} \quad (27)$$

Dividing this by V_h then gives an explicit expression for the containment time, t_c .

To obtain the area, it is only necessary to substitute in the parametric equations for the upper and lower portions of the final containment boundary

$$x_i = h(u_i) \cos u_i \quad y_i = h(u_i) \sin u_i \quad (28)$$

the expression which follows from (25),

$$h(u_i) = h_0 e^{\left(\pm \frac{\pi - u_i}{\sqrt{P_i^2 - 1}} \right)} \quad (29)$$

The upper (lower) sign is used for $i = 1$ ($i = 2$). Since this represents the containment perimeter in terms of the parameters u_i , it is convenient to modify (7) to express the area in terms of this same representation,

$$Area = \int_{\pi}^{u_c} y_1(u_1) \frac{dx_1}{du_1} - \int_{\pi}^{u_c + 2\pi} y_2(u_2) \frac{dx_2}{du_2} \quad (30)$$

where u_c is obtained from (25) by substituting h_c , as given by (26), for h ,

$$u_c = \left[\frac{\sqrt{P_2^2 - 1} - \sqrt{P_1^2 - 1}}{\sqrt{P_2^2 - 1} + \sqrt{P_1^2 - 1}} \right] \pi \quad (31)$$

While the integrations in (30) can be carried out in closed form for any $P_i > 1$, the results simplify considerably for the case where the resources are divided equally between the upper and lower portions of the boundary, i.e., for $P_1 = P_2 = P$. The containment area is then just twice the area of the upper portion, so, dropping the subscript 1 on x , y , and u , one has

$$Area = 2 \int_{\pi}^0 y(u) \frac{dx}{du} du = h_0^2 e^{2q\pi} I \quad (32)$$

where

$$q = \frac{1}{\sqrt{P^2 - 1}}$$

and

$$\begin{aligned} I &= \int_0^{\pi} e^{-2qu} [q \sin(2u) - \cos(2u) + 1] du \\ &= -\frac{1}{2} \left[e^{-2qu} \left(\sin(2u) + \frac{1}{q} \right) \right]_0^{\pi} = \frac{(1 - e^{-2\pi q})}{2q} \end{aligned} \quad (33)$$

The final result is

$$Area = \frac{h_0^2 [e^{2q\pi} - 1]}{2q} \quad (34)$$

In the limit where P is very large (and hence q approaches 0), (34) reduces to $\pi(h_0)^2$, as it should.

Note that t_c and the area depend very sensitively (exponentially) on $q = \frac{1}{\sqrt{P^2 - 1}}$. This same sensitivity is evident in

the more complicated cases discussed below where $\epsilon > 0$ and the P_i are variable (cf. Figure 4). Moreover, the dependence of t_c and $Area$ on ϵ is very weak compared to the dependence on the P_i (cf. Figure 5).

Direct Head Attack

The analysis for this case is quite similar to that for the direct tail attack. The functions u_i are again determined by

solving (10); the resulting fire perimeter, for contained fires is given by (5) and (6); $D = 0$ determines h_c and hence t_c ; and the area of the contained fire is calculated from (7). There are, however, some sign changes. Consider first the upper boundary, for which u starts at 0 and increases. On the right side of (10) the first term in the numerator is still positive but now $\frac{du_1}{dh}$ should also be positive, since the head of the line-building effort must proceed in a counter-clockwise direction (i.e., increasing u) as t and h increase. If the magnitude of the second term in the numerator is less than that of the first term, the proper sign of $\frac{du_1}{dh}$ can be achieved with either choice of sign. However, choosing the minus sign constrains P_i to lie within narrow limits: if it drops to the value P_n given by (11), the argument of the square root will become negative, and the integration cannot proceed; if it increases above the value $\sqrt{X^2 + Y^2}$, $\frac{du}{dh}$ will change sign, and again the integration fails.

It is therefore appropriate to use the plus sign in (10) for the upper boundary. For the lower portion of the boundary, where u decreases from an initial value 2π , similar arguments lead to the choice of the minus sign on the square root. With these sign choices, the sign of $\frac{du}{dh}$ is fixed for each portion of the boundary, and the only difficulty which can arise is if P drops to P_n and the argument of the square root becomes negative. Should this happen, the integration is terminated, and the fire is classified as having escaped.

Parallel Attack

On a particularly hot or fast-spreading fire, firefighters will often rely on an alternate set of tactics that reduces their exposure to death or injury while still allowing them to achieve fire containment. These tactics involve building fireline parallel to but offset from the expanding perimeter, with or without the setting of backfires ("firing out") along the way. Assume that firefighters arrive at a fire whose free-burning boundary is given by Equation (1), and begin constructing line at a distance, L , from the fire. Assume further that the minimum distance between the free-burning fire perimeter and the point of current line-building activity (i.e., the location of the fire crews at time t) is constrained to be always L . This requirement can most easily be formulated by introducing the concept of the super fbfb, defined as follows.

Consider a time t , when the fbfb consists of the locus of points whose coordinates are given by (1). For any point Q on the fbfb, characterized by a particular value of u , let Q' be the point which lies on the outward normal to the fbfb, at a distance L from Q . Define the super fbfb at time t to be the locus of all such points Q' . Then the problem of indirect or parallel attack is equivalent to the problem of direct attack on an imaginary fire whose fbfb coincides with the super fbfb of the actual fire being considered.

To obtain equations for the super fbfb, consider a point Q on the fbfb characterized by a value u (Figure 3). Let $\psi(u)$ be

the angle between the outward normal to the fbfb at Q and the x axis, measured in a counter-clockwise direction from the positive x axis. Then the coordinates of the corresponding point Q' on the super fbfb will be

$$x = hX(u, \epsilon) + L \cos \psi \quad \text{and} \quad y = hY(u, \epsilon) + L \sin \psi \quad (35)$$

so (35) constitutes a parametric representation of the super fbfb associated with the fbfb described by (1). To derive an expression for ψ , recall that the slope of the tangent line to the fbfb at Q is obtained from (1) by computing $\frac{dy}{dx}$ with h held constant, i.e., the slope of the tangent line is $\frac{Y_u}{X_u}$. The slope of the normal is then the negative reciprocal of this, i.e.,

$$\tan \psi = -\frac{X_u}{Y_u} \quad (36)$$

or, equivalently,

$$\sin \psi = -\frac{X_u}{\sqrt{X_u^2 + Y_u^2}} \quad \cos \psi = \frac{Y_u}{\sqrt{X_u^2 + Y_u^2}} \quad (37)$$

The analysis of the parallel attack case closely parallels that given above for the direct attack, with (1) replaced by (35). Again, the crux of the problem is the determination of the functions $u_i(h)$, the requirement being that the velocity with which line can be built match the velocity of the point on the super fbfb where line is being constructed. This condition, which is expressed by (8) for the upper part of the super fbfb, becomes

$$\left(\frac{dh}{dt} X + \frac{du_1}{dt} [hX_u - L\psi_u(u_1) \sin \psi(u_1)] \right)^2 + \left(\frac{dh}{dt} Y + \frac{du_1}{dt} [hY_u - L\psi_u(u_1) \cos \psi(u_1)] \right)^2 = V_1^2 \quad (38)$$

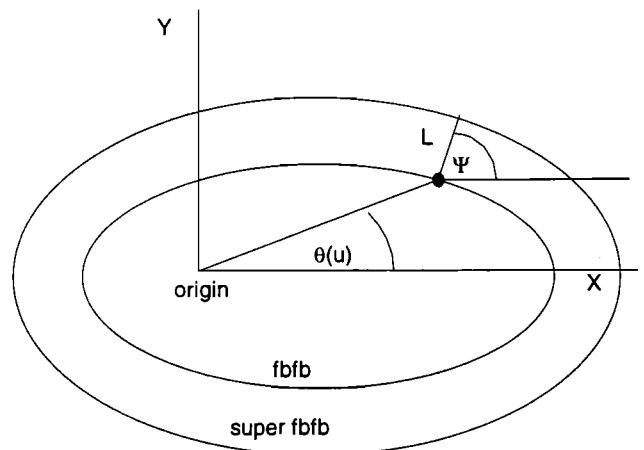


Figure 3. Free-burning fire boundary and super free-burning fire boundary on which fireline is constructed in a parallel attack.

Using (37) and, as before, taking h as independent variable in place of t , this can be rewritten in the form

$$\left(X + \frac{du_1}{dh} X_u H_1\right)^2 + \left(Y + \frac{du_1}{dh} Y_u H_1\right)^2 = P_1^2 \quad (39)$$

where H_1 is defined by

$$H_1 \equiv h + \frac{L\Psi_u(u_1)}{\sqrt{X_u^2 + Y_u^2}} \quad (40)$$

Like (9), (39) is a quadratic equation for $\frac{du_1}{dh}$. In fact, (39) differs from (9) *only* in the replacement of h by H_1 on the left-hand side, so the solution to (39) and to the analogous equation for the lower portion of the super fbfb is just obtained by substituting for h in (10) the quantity

$$H_i \equiv h + \frac{L\Psi_u(u_i)}{\sqrt{X_u^2 + Y_u^2}} \quad (41)$$

In short, $\frac{du_i}{dh}$ for the parallel attack problem is given by

$$\frac{du_i}{dh} = \frac{-(XX_u + YY_u) \pm \sqrt{P_i^2(X_u^2 + Y_u^2) - (X_u Y - Y_u X)^2}}{\left[h + L\Psi_u(u_i) / \sqrt{X_u^2 + Y_u^2}\right] (X_u^2 + Y_u^2)} \quad (42)$$

the choice of signs being the same as for the direct attack. For example, for tail attack, the negative sign is to be used for the upper portion of the boundary ($i = 1$) and the positive sign for the lower portion ($i = 2$).

From this point on, the analysis proceeds exactly as for the direct attack, and most of the discussion of that case applies to parallel attack. However, even for the case of constant P_i the solution of (42) cannot be reduced to a quadrature since the right-hand side is no longer the quotient of a function of u and a function of h .

As with direct attack, the example of an elliptical fbfb is of special interest. With X and Y given by (22), it follows from (36) that

$$\tan \psi = \frac{\tan u}{\sqrt{1 - \epsilon^2}} \quad (43)$$

Differentiating this with respect to u and employing elementary trigonometric identities gives

$$\Psi_u = \frac{d\Psi}{du} = \frac{\sqrt{1 - \epsilon^2}}{1 - \epsilon^2 \cos^2 u} \quad (44)$$

Furthermore,

$$X_u^2 + Y_u^2 = \frac{1 - \epsilon^2 \cos^2 u}{1 + \epsilon^2} \quad (45)$$

from which it follows that

$$H_i = h + \frac{LA}{\sqrt{1 - \epsilon^2 \cos^2 u_i}} \quad (46)$$

Substituting this H_i in place of h on the right-hand side of (23) gives the fundamental equation for $\frac{du_i}{dh}$ in the case of parallel attack on a fire with an elliptical fbfb.

Summary of the Algorithm

The steps for implementing the self-consistent algorithm are presented here for the case of direct tail attack. Slight modifications of these steps in terms of sign and function are sufficient to characterize the other kinds of attack discussed earlier. Converting this algorithm into a C, Pascal, or FORTRAN computer program is relatively straightforward for those familiar with the processing of array data structures and the implementation of numerical algorithms of the type found in Press (1986). Definitions of the variables referenced in this summary are listed in Table 1.

1. Choose a shape for the fbfb, based on physical attributes of the fire site, weather conditions, etc. This amounts to a choice of the functions X and Y in (1).
2. Determine the time dependence of the fbfb scale, i.e., the function $h(t)$ in (1), from which follows the rate of advance,

$$V_h = \frac{dh}{dt}.$$

3. Identify the productivity and arrival times of the line-building resources at the upper and lower boundaries. This determines the time t_0 of initial attack and the functions

$$V_i(t) \text{ or } V_i(h) \text{ and hence } P_i = \frac{V_i}{V_h}.$$

4. Choose a time step Δt and, correspondingly, an h step $\Delta h = V_h \Delta t$ for the integration of (10) and advance the u_i using standard techniques such as Runge-Kutta integration, thus generating the functions $u_i(h)$. Also specify the maximum allowable time, t_{\max} .
5. At each integration step, calculate the distance D between Q_1 and Q_2 and terminate the integration when $D = 0$ (classifying the fire as contained) or when t exceeds t_{\max} (classifying the fire as escaped).

6. If, at any time step, $\frac{du_i}{dh}$ changes sign (i.e., if $\frac{du_1}{dh}$ goes positive or $\frac{du_2}{dh}$ goes negative), terminate the integration and classify the fire as escaped.

Table 1. Definition of expressions used in the summary of the self-consistent algorithm for simulating initial attack.

Expression	Definition
$X(u,\epsilon), Y(u,\epsilon)$	Parametric definition of the x and y coordinates in a Cartesian system given the angular variable u and eccentricity ϵ and unit scale; these are multiplied by $h(t)$ to obtain x and y coordinates.
$V_h = \frac{dh}{dt}$	In general, this is the forward rate of spread of the fire, which may, or may not, be constant.
t_0	The time between fire ignition and commencement of initial attack efforts.
$V_i(t)$ or $V_i(h)$	The aggregate line-building rate, in units of linear distance per time, on the "upper" ($i = 1$) and "lower" ($i = 2$) containment boundaries (in a plan view) as functions of time since fire ignition (t) or distance of travel from the fire origin to the leading edge of the fire.
P_i	The ratio of the line building rate for boundary i to the expansion rate of the free burning fire, V_h .
$\Delta t, \Delta h$	The time and h increments used in the computation of the Runge Kutta solution for the differential equation for u_i .
$u_i(h)$	The angular variable that tracks the position of line building activity for any given time t , or by parametric extension, h : the distance traveled by the head of the fire (note that in the case of head attack, h represents the distance that would have been traveled had linebuilding not blocked forward movement).
Q_1 and Q_2	At any given time (or h) step, the locations at which active linebuilding is underway on the upper and lower containment boundaries.
$\frac{du_i}{dh}$	The change in the angular variable u with respect to the change in head position h for boundary i ; this is the differential equation that is integrated via Runge-Kutta to trace out the containment boundary.

7. For contained fires, the containment time t_c is the time at which $D=0$. The parametric equations of the fire perimeter are given by (5) and (6) and the burned area is given by (7).

Application

A Runge-Kutta solution of (23) was encoded in Pascal and matched with an interactive shell to facilitate the simulation of fires with different spread rates, eccentricities, strategies, tactics, and patterns of resource arrivals. This PC-based program, the Fire Containment Algorithm Tester (FCAT),⁵ allows entry of arrival times and production rates for as many as 125 firefighting resources; forward rate of spread (V_h); initial size; choice of tactics (head or tail attack); choice of strategy (direct or parallel attack); and, if parallel attack is selected, specification of the offset distance (L). If the simulated fire does not escape initial attack, outputs from FCAT include the final size (*Area*), containment time (t_c), the number of resources utilized, and a graphic representation of the contained perimeter. Otherwise, the program simply returns "escape." For purposes of comparison, FCAT also reports these same quantities as calculated via the Simple Method currently used in fire planning models [such as CFES version 1 (Fried and Gillies 1988b, Fried et al. 1987) and NFMAS (USDA Forest Service 1985)], where perimeter growth and linebuilding are assumed to be independent, non-interacting processes. FCAT successfully duplicated the results of the Simple Method initial attack scenarios reported by Mees (1985).

The characteristics of the functional dependence of *Area* and T_c on ϵ and P_i can most easily be illustrated for the case of direct, tail attack on elliptical fires, with constant P_i (with

$P_1 = P_2 = P$), and unit initial size. FCAT simulations were in agreement with tables of such relationships published by Bratten (1978); however, FCAT's ability to handle the more realistic case of variable P_i and to treat parallel attack makes it a far more useful tool than containment tables. Simulations for a range of P values and three different eccentricities (0, 0.55, and 0.87) corresponding to length to width ratios (A/B) of 1.0, 1.2, and 2.0 reveal dramatically diminishing returns to increases in P . For any choice of eccentricity, an increase in P from 1.2 to 2.2 results in a reduction in fire size by as much as two orders of magnitude, yet a further increase to 3.2 reduces area by less than 50% (Figure 4). Furthermore, the choice of eccentricity has a declining impact on area as P increases. The impacts of increases in P on T_c are only somewhat less dramatic (Figure 5); however, here there is an early apparent convergence across eccentricities, and in fact, a "cross-over" that results in a length-to-width ratio of 1.2 having the lowest containment time at high P .

Comparisons of the *Area:P* relationships generated by our General Formulation Method with those generated by the Simple Method indicate that the latter dramatically overestimates fire size in all cases (Figure 6). For example, for a fire with an eccentricity of 0 (a circular fbfb), three times as much fireline building capability was required to prevent an escape when calculated by the Simple Method. Under head attack scenarios on noncircular fires, these differences are even more dramatic.

To obtain a comparison of the Simple and General Formulation methods under more realistic conditions, 30 so-called "representative" fires with "historical" spread rates from a grass-fuel fire management analysis zone in the California Department of Forestry and Fire Protection's

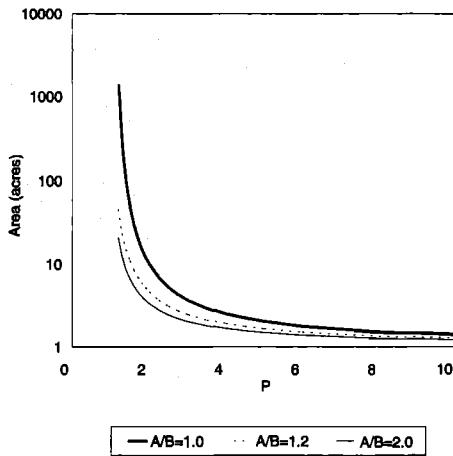


Figure 4. Area of contained fires burning with elliptical fbb's and length to width (A/B) ratios 1.0, 1.2, and 2.0, attacked from the tail, for a range of P . For initial size of 1 ac, the final size can be read from the y axis directly as acres.

Santa Clara ranger unit (a five-county region in the San Francisco Bay Area) were simulated with FCAT. Five different locations (representing a range of resource response times and fireline productivity potentials) and a range of historical spread rates (8 to 47 chains per hour) formed the basis of these 30 representative fires. Assuming direct, tail attack on all fires, a 2:1 elliptical shape, and an initial size of 0.01 ac, the differences between the two methods are less than for the simple, constant P case, probably because some of the firefighting capacity arrives later in the firefighting effort and thus has less impact on the overall *spread* of the fire (some of the perimeter would have already been contained by early arrivals). While the Simple Method results in slight overestimates of area and containment time (t_c) for fires with spread rates that are slow in relation to fireline construction rate (and tend to be small), the error increases significantly for faster spreading fires (which tend to have larger values for containment size) as shown in the comparison for the medium and high fire dispatch level (FDL) fires at the Orestimba representative fire location (Tables 2 and 3). When a head attack is assumed for low and medium FDL fires, the differences in model results are even more pronounced.

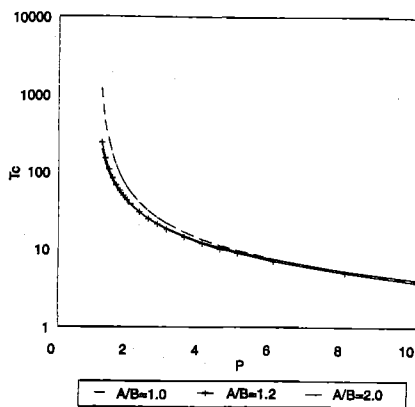


Figure 5. Containment time T_c (in units of h_0/V_h) of contained fires burning with elliptical fbb's and length to width ratios 1.0, 1.2, and 2.0, attacked from the tail, for a range of values of P .

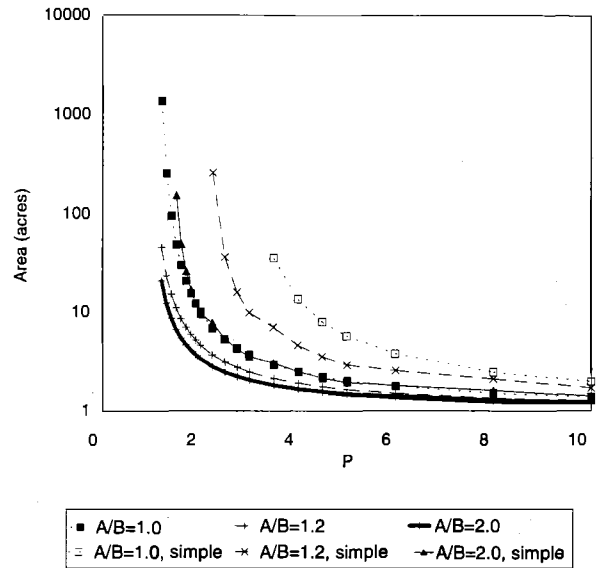


Figure 6. Area of contained fires burning with elliptical fbb's and length to width ratios 1.0, 1.2, and 2.0 for a range of values of P as predicted by the Simple Method and our General Formulation algorithm. The P value corresponding to the leftmost point on each curve is the lowest productivity which will lead to containment for the given A/B. For initial size of 1 ac, the final size can be read from the y axis directly as acres.

Simulations of parallel attack with a five-chain offset produced fires with sizes that were somewhat greater than for direct attack, but much less than when computed using the Simple Method. As might be expected, the simulations show that the total perimeter length of the confined fire is not much greater in the case of parallel attack than it is for direct attack, provided the size of the offset in the former case is small compared to the dimensions of the confined area. Thus, it is not surprising that the percentage differences in confinement times for these two approaches are quite small. The differences in the confined areas for the two cases are substantial (ranging from 25 to 60% for the examples given in Table 2). To a first approximation, we would expect the area in the case of parallel attack to be greater by an amount roughly equal to the product of the perimeter of the confined fire and the offset. A comparison of the area (for parallel attack) estimated in this way with the result of the simulation is also shown in Table 2. It appears from this comparison, as well as from a number of other simulations we have run, that this rough estimate is a useful way of assessing the difference in area for the two methods of attack.

Discussion

Our General Formulation containment algorithm yields more realistic assessments of the area of contained fires than does the Simple Method underlying existing initial attack simulators. Indeed, one of the primary complaints of the fire protection planners and firefighters who rely on existing simulation models has been that they perceive the fire areas and frequency of escapes projected by those models to be unbelievably large relative to historical fire statistics and their own experience. While an ellipse may

well be a good choice for representing a free burning fire, it is a poor choice for representing the actual containment boundary, and this is a critical deficiency of the Simple Method.

The greater the fraction of fireline building resources which arrive early in the attack on a fire, the larger the error obtained using the Simple Method. This has serious implications for modeling the contributions of water dropping aircraft, which can be represented in FCAT or any simulation model based on the General Formulation as a short (1 minute or less) burst of very high productivity, P , rising briefly from a baseline level that represents the productivity of all ground resources, to a very high ratio, then returning to the baseline level. The first air tankers often arrive early in the course of the fire, sometimes even before any ground-based resources have arrived at the incident, and with their ability to lay down a near instantaneous strip of "wet" fireline, are in an excellent position to produce a significant decrease in the length of actively expanding fire perimeter. This aspect of their effectiveness is well represented by our General Formulation and completely ignored by the Simple Method.

We ran a series of simulations, all with the same average line-building rate but with different sequences of arrivals and linebuilding rates, to examine the limitations of assuming a constant line-building rate. Comparisons of the sizes of fires modeled under variable production rates with those modeled under the constant (time weighted average) production rate assumption included in some of the earlier papers indicated that the assumption of constant production rates exerts a bias on calculated fire size whenever there is a mixture of high and low productivity resources, and the arrivals are not evenly distributed over time. The direction of the bias depends on whether high productivity resources arrive towards the beginning or end of the initial attack. For example, having a high productivity resource (e.g., a bulldozer) arrive near the end of the initial attack will have less impact on fire size than would be assumed using a time-weighted average production rate for the entire initial attack. The error can be particularly large (greater than a factor of two) when resources that

produce fireline for short periods are included (e.g., fire engines that run out of water, and thus drop in productivity, and air tanker or helicopter water/retardant drops, which are handled in this formulation as if they were a short burst of very high line-building productivity). The ability to model variable line production is important in situations where the first-arriving resources are insufficient to safely attack the fire. This is immediately detected with our General Formulation Method, because one of the mathematical conditions given above for terminating the calculation and classifying the fires as "escaped" will then be satisfied. In a calculation using constant (average) line construction rates, this situation might easily go undetected. An operational advantage of the variable line-building assumption is the elimination of the need to calculate an average production rate; because we do not know the containment time in advance, it is difficult to select the time period over which to calculate the average production rate.

Mees (1985) reported relatively small differences in fire area between the Simple Method and his Complex Method for all but extreme fires, and, on this basis, virtually dismissed the importance of the Complex Method. However, it is precisely the extreme fires that fire planners must be able to accurately model, as these are the fires that are most likely to exceed the firefighting capacity of the firefighting organization and become the large, damaging wildfires that consume whole neighborhoods and about which many people care a great deal. Furthermore, the researchers who have sought to model fire containment heretofore have focused on the kinds of wildfires and firefighting tactics that occur on lands managed by the USDA Forest Service. In sharp contrast with fires that occur on lands protected by the Forest Service, the typical wildfire for which CDF has responsibility tends to burn rapidly (typically in flashy fuels composed of dried grass and brush rather than in slow burning forest), threaten homes and other developments within minutes of ignition (rather than only uninhabited public land), and receive an aggressive response from water pumping engines and water dropping aircraft within 10 to 20 minutes (instead of 2 to 4 hours). These additional considerations render the

Table 2. General Formulation, direct attack; General Formulation, parallel attack; and the Simple method. Perimeter (in chains) calculated for the direct attack case can be multiplied by the five-chain parallel offset to provide estimated areas for the parallel case that are close to the simulation results for parallel attack. The eight simulated fires are representative of those occurring in the annual grass, low population density analysis zone of the Santa Clara ranger unit near Orestimba. The last four rows in the table correspond to fires with lesser spread rates for which a head attack tactic may be appropriate, and which typically do not require parallel attack.

ROS (chains/hr)	FDL	Attack	General formulation (direct)			General formulation (parallel)			Simple method	
			Area (ac)	t_c (min.)	Perim (chains)	Area (ac)	t_c (min.)	Est. area (ac)	Area (ac)	t_c (min.)
26.8	Medium	Tail	164	175	180	262	178	254	339	193
33.6	Medium	Tail	460	259	316	629	263	618	2,633	431
40.3	High	Tail	750	271	397	960	274	948	3,486	413
47.0	High	Tail	1,963	386	697	2,319	390	2,311	149,228	2,321
7.8	Low	Head	4	86	NA	NA	NA	NA	5.5	82
14.7	Low	Head	24	128	NA	NA	NA	NA	44	126
26.8	Medium	Head	82	144	NA	NA	NA	NA	339	193
33.6	Medium	Head	144	164	NA	NA	NA	NA	2,633	431

Table 3. Dispatch List for Orestimba, Santa Clara ranger unit, California, containing the order of arrival, the type of firefighting resource, the delay (following report of the fire) before a resource arrives on the scene, the full production rate expected for the firefighting resource (the software allocates half of this to each fire flank), and the minimum Fire Dispatch Level at which the resource would be dispatched. Production rates for firefighting resources deployed on the ground are stated in chains per hour (cph); production rates for air tanker and helicopter drops of water and retardant are shown in chains (ch) but are converted by the software into an equivalent production rate that is sustained for one minute. The dropoff phenomenon is ignored in this example.

Seq. #	Resource type	Arrival time (min.)	Production rate (chains/hr)	Minimum FDL for dispatch
1	Air tanker drop	27	8.0 ch	Low
2	Air tanker drop	27	8.0 ch	Medium
3	Helicopter crew	41	6.3 cph	Low
4	Helicopter drop	41	3.0 ch	Low
5	Engine	45	3.0 cph	Low
6	Engine	45	3.0 cph	Low
7	Engine	49	3.0 cph	Low
8	Helicopter drop	61	3.0 ch	Low
9	Engine	64	3.0 cph	Low
10	Engine	64	3.0 cph	Low
11	Engine	64	3.0 cph	Low
12	Engine	70	3.0 cph	High
13	Engine	70	3.0 cph	High
14	Engine	79	3.0 cph	Low
15	Bulldozer	80	18.0 cph	Medium
16	Air tanker drop	81	8.0 ch	Low
17	Air tanker drop	81	8.0 ch	Medium
18	Helicopter drop	81	3.0 ch	Low
19	Engine	94	3.0 cph	Low
20	Bulldozer	100	18.0 cph	Low
21	Helicopter drop	101	3.0 ch	Low
22	Engine	105	13.3 cph	Low
23	Engine	105	3.0 cph	Low
24	Engine	105	3.0 cph	Low
25	Engine	110	3.0 cph	Low
26	Engine	110	3.0 cph	Low
27	Engine	110	3.0 cph	Low
28	Engine	110	3.0 cph	Low
29	Engine	110	3.0 cph	Low
30	Bulldozer	118	18.0 cph	High

Simple Method particularly unsuitable for simulating wild-fire containment on CDF protected lands. Fortunately, computing power is no longer limiting, so that the use of the General Formulation is quite feasible, even in simulation models, like CFES version 2 (Fried and Gilless 1988a), which simulate thousands of individual fires.

Literature Cited

- ALBINI, F.A., G.N. KOROVIN, AND E.H. GOROVAYA. 1978. Mathematical analysis of forest fire suppression. USDA For. Serv. Res. Pap. INT-207. 20 p.
- ANDERSON, H.E. 1983. Predicting wind-driven wild land fire size and shape. USDA For. Serv. Res. Pap. INT-305. 26 p.
- ANDERSON, D.H. 1989. A mathematical model for fire containment. Can. J. For. Res. 19:997-1003.
- BRATTEN, F.W. 1978. Containment tables for initial attack on forest fires. Fire Tech. 14(4):297-303.
- FRIED, J.S., AND J.K. GILLESS. 1988a. Modification of an initial attack simulation model to include stochastic components. P. 235-246 in Proc. 1988 Symp. on Systems analysis in forest resources. USDA For. Serv. Gen. Tech. Rep. RM-161.
- FRIED, J.S., AND J.K. GILLESS. 1988b. The California fire economics simulator initial attack module (CFES-IAM): MS-DOS Version 1.11 User's Guide. Bull. 1925. Div. of Agric. and Natur. Resour., University of California, Berkeley. 84 p.
- FRIED, J.S., J.K. GILLESS, AND R.E. MARTIN. 1987. CFES—The California Fire Economics Simulator: A computerized system for wildland fire protection planning. P. 212-217 in Proc. Symp. on Wildland Fire 2000. USDA For. Serv. Gen. Tech. Rep. PSW-101.
- MEES, R.M. 1985. Simulating initial attack with two fire containment models. USDA For. Serv. Res. Note PSW-378. 7 p.
- PRESS, W.H., B.P. FLANNERY, S.A. TEUKOLSKY, AND W.T. VETTERLING. 1986. Numerical recipes: The art of scientific computing.
- USDA Forest Service. 1985. National fire management analysis system users' guide of the initial action assessment model (FPL-IAA2.2). USDA For. Serv., Wash., DC.

Endnotes

- For example, if the shape is chosen to be a single ellipse (Mees 1985), ϵ is just the eccentricity of that ellipse. For a double ellipse (Anderson 1983), ϵ stands for four parameters: the eccentricities of the two ellipses, the ratio of their major axes, and the ratio of one major axis to the distance between their centers. For the families of curves chosen by Albini, et al., ϵ represents three parameters: their exponent

n and the ratios of the flanking and backward advance rates, V_f and V_B , to the forward advance rate, V_F . The parameter u is a monotonically increasing function of θ , the angle between a line from the origin to the head of the fire and a line from the origin to the point whose coordinates are given by (1) (cf. Figure 1). We could, for example, choose $u = \theta$ but as will be seen in the example of an elliptical fbfb, other choices can significantly simplify the algebra.

- 2 Determination of $\frac{du}{dt}$ is equivalent to choosing the "angle of attack" $\alpha(t)$, i.e., the angle which the direction of the line-building effort makes with the x axis. For instance, if u is constant, $\frac{du}{dt} = 0$, then (7.1) gives $v = v_0 = v_h \sqrt{X^2 + Y^2}$ and the point given by (1) simply moves radially outward along the line from the origin to that point. If V_1 , the line-building rate on the upper boundary at time t , is just equal to v_0 , then the direction of line building is radially outward ($\alpha = \theta$), the fire continues to expand freely at all smaller values of θ , and there is no progress towards containment. The value of $\frac{du}{dt}$ which minimizes v is:

$$\frac{du}{dt} = \frac{-V_h}{h} \frac{XX_u + YY_u}{X_u^2 + Y_u^2} = \frac{-V_h}{2h} \left(\frac{d}{du} \right) (X^2 + Y^2)$$

This is positive (since $X^2 + Y^2$ increases with decreasing u and θ) and the corresponding minimum value of v is:

$$v_{\min} = \frac{V_h |XY_u - YX_u|}{\sqrt{X_u^2 + Y_u^2}}$$

If V_1 is just equal to v_{\min} , then the line-building direction is normal to the fbfb, u and θ increase with time, and there is negative progress towards containment (although containment may still be achieved if V_1 subsequently becomes large enough). So long as V_1 is greater than v_0 , α can be less than θ . Then u and θ decrease with time and there is progress towards containment. Since v increases as α

decreases below θ (and the magnitude of $\frac{du}{dt}$ increases),

the best choice of α , and hence of $\frac{du}{dt}$, is that for which v is as large as it can be, namely $v = V_1$.

- 3 This follows from an analysis of the right-hand side of (10). (N.B. This discussion is fairly technical and can be omitted by readers not concerned with the mathematical details.) For $i = 1$, i.e., on the upper part of the boundary, the first term in the numerator is equal to

$$-\frac{1}{2} \left[\frac{d(X^2 + Y^2)}{du} \right]$$

This quantity is positive, since $\sqrt{X^2 + Y^2}$, the distance from the origin to a point on the upper part of the fbfb, increases as the point moves in a clockwise direction, from tail to head, and u decreases, from π to 0.

This increasing character of $\sqrt{X^2 + Y^2}$ can be formally and explicitly demonstrated for the specific fbfb shapes usually considered, e.g., the ellipse (Mees), the double ellipse (Anderson), and the family of shapes used by Albini, et al. More generally, it can be seen intuitively to hold for physically sensible choices of fbfb shape.

The fact that $\frac{du_1}{dh}$ must be negative (so that the head of the line-building effort proceeds in a clockwise direction as t , and hence h , increases) accounts for the choice of the minus sign on the square root in (10) for $i = 1$. So long as the magnitude of the square root exceeds $|XX_u + YY_u|$, $\frac{du_1}{dh}$ will remain negative, and the integration proceeds without difficulty. This will be the case if P_1 is large enough, but if at some time P_1 becomes too small, $\frac{du_1}{dh}$ may pass through zero. The model then fails mathematically because the portion of the fire boundary near the line-building point is no longer describable by the initially chosen fbfb shape. The fire-fighting effort also fails, since the fire can then burn around the head of the line-building point and engulf the fire fighters. As noted above, such a fire is classified as

having escaped. From (9), $\frac{du_1}{dh} = 0$ implies

$P_1 = \sqrt{X^2 + Y^2}$, which is equivalent to the statement that V_1 equals the velocity U_1 of a point on the expanding fbfb corresponding to fixed u . For such a point,

$$\frac{dx}{dt} = X \frac{dh}{dt}, \quad \frac{dy}{dt} = Y \frac{dh}{dt}$$

and so

$$U_1 = \sqrt{\left(\frac{dx}{dt} \right)^2 + \left(\frac{dy}{dt} \right)^2} = V_h \sqrt{X^2 + Y^2}$$

Of course, the above discussion for the upper portion of the boundary applies as well to the lower part, with suitable sign changes. On the lower portion of the fbfb, the first term in the numerator of (10) is negative, since the distance $\sqrt{X^2 + Y^2}$ from the origin to a point on that boundary, increases as the point moves in a counter-clockwise direction from tail to head and u_2 increases from π to 2π . However, for this portion $\frac{du_2}{dh}$ must be positive (since the head of the line-building effort must move in a counter-clockwise direction as t and h increase), and so the positive sign must be chosen for the square root in (10) when $i = 2$. Again, the fire is classified as having escaped if, at any step, P_2 is less

than $\sqrt{X^2 + Y^2}$.

In addition to the vanishing of $\frac{du}{dh}$, it might be supposed that the integration procedure would encounter difficulty if at some point P_i becomes so small that the argument of the square root in (10) goes negative. From (10) it can be seen that this occurs if P_i falls below the value

$$P_n = \frac{(X_u Y - Y_u X)}{\sqrt{X_u^2 + Y_u^2}} \quad (11)$$

which can be shown to correspond to having V_i less than the rate of advance of the fbfb in the direction normal to the boundary. However, P_n is less than $\sqrt{X^2 + Y^2}$, since

$$P_n^2 - (X^2 + Y^2) = -\frac{(XX_u + YY_u)^2}{X_u^2 + Y_u^2} < 0 \quad (12)$$

so this problem can arise only for values of P_i smaller than that which makes $\frac{du_i}{dh}$ change sign. Before P_i drops to P_n , the fire will have been classified as escaped and the integration halted.

⁴ The canonical equation for an ellipse in a coordinate system for which the origin is at the center of the ellipse is

$$\left(\frac{x}{a}\right)^2 + \left(\frac{y}{b}\right)^2 = 1 \quad (17)$$

where a and b are the major and minor semi-axes, and

$$\epsilon = \sqrt{1 - \left(\frac{b}{a}\right)^2}$$

A parametric representation for the ellipse is given by

$$x = a \cos u \quad y = b \sin u \quad 0 \leq u \leq 2\pi \quad (18)$$

and it is clear that (18) satisfies (17).

Alternatively, an ellipse can be defined as the locus of points for which the sum of the distances from two given points, the foci, is equal to some constant c . Expressing this analytically and choosing the foci to lie on the x axis at a distance f from the center leads to an equation of the form (17) with

$$a = \frac{c}{2}, \quad b = \sqrt{a^2 - f^2} \quad \text{and} \quad f = \epsilon a \quad (19)$$

For the scale factor h to be used in (1) it is convenient to take the distance from the left-hand focus (the origin of the fire) to the right-hand end of the ellipse (the head of the fire), i.e., to choose

$$h = a + f = a(e + 1) \quad (20)$$

⁵ FCAT, which runs on MS-DOS based PCs, is available for downloading via World Wide Web at the following URL:
<http://www.for.msus.edu/~jeremy/programs/fcat.htm>